Impact of precipitation and increasing temperatures on drought trends in eastern Africa

Sarah F. Kew[1], Sjoukje Y. Philip[1], Mathias Hauser[2], Mike Hobbins[3,4], Niko Wanders[5], Geert Jan van Oldenborgh[6], Karin van der Wiel[6], Ted I.E. Veldkamp[1], Joyce Kimutai[7], Chris Funk[8,9], and Friederike E.L. Otto[10]

[1]Institute for Environmental Studies, Vrije Universiteit, Amsterdam, The Netherlands
[2]Institute for Atmospheric and Climate Science, ETH Zurich, Zurich, Switzerland
[3]Cooperative Institute for Research in Environmental Sciences, University of Colorado Boulder, Boulder, Colorado
[4]Physical Sciences Division, NOAA/Earth System Research Laboratory, Boulder, Colorado
[5]Department of Physical Geography, Utrecht University, Utrecht, the Netherlands
[6]Royal Netherlands Meteorological Institute (KNMI), De Bilt, The Netherlands
[7]Kenya Meteorological Department, Nairobi, Kenya
[8]U.S. Geological Survey Center for Earth Resources Observation and Science, Sioux Falls, South Dakota
[9]University of California, Santa Barbara, Santa Barbara, California
[10]School of Geography and the Environment, University of Oxford, Oxford, UK

Correspondence: Sarah F. Kew (sarah.kew@knmi.nl)

Abstract. In eastern Africa droughts can cause crop failure and lead to food insecurity. With increasing temperatures, there is an a priori assumption that droughts are becoming more severe, however, the link between droughts and climate change is not sufficiently understood. In the current study we investigate trends in long-term agricultural drought and the influence of increasing temperatures and precipitation deficits.

Using a combination of models and observational datasets, we studied trends, spanning the period from 1900 (to represent the pre-industrial era) to 2018, for six regions in eastern Africa in four drought-related annually averaged variables — soil moisture, precipitation, temperature and, as a measure of evaporative demand, potential evapotranspiration (PET). In standardized soil moisture data, we found no discernible trends. Precipitation was found to have a stronger influence on soil moisture variability than temperature or PET, especially in the drier, or water-limited, study regions. The error margins on precipitation-trend estimates are however large and no clear trend is evident. We find significant positive trends in local temperatures. However, the influence of these on soil moisture annual trends appears limited. The trends in PET are predominantly positive, but we do not find strong relations between PET and soil moisture trends. Nevertheless, the PET-trend results can still be of interest for irrigation purposes because it is PET that determines the maximum evaporation rate.

We conclude that, until now, the impact of increasing local temperatures on agricultural drought in eastern Africa is limited and we recommend that any soil moisture analysis be supplemented by an analysis of precipitation deficit.

Copyright statement. TEXT

1 Introduction

In eastern Africa, drought has occurred throughout known history and the phenomenon has incurred significant impacts on the agricultural sector and the economy, particularly thorough threats to food security. It is therefore important to examine the role of anthropogenic climate change in drought, particularly in the face of the large-scale droughts of 2010/11, 2014 and 2015 in Ethiopia, and the 2016/17 drought in Somalia, Kenya, parts of Ethiopia and surrounding countries, which have recently raised the spectre of climate change as a risk multiplier in the region.

Droughts are triggered and maintained by a number of factors and their interactions, including meteorological forcings and variability, soil and vegetation feedbacks and human factors such as agricultural practices and management choices, including irrigation and grazing density (van Loon et al., 2016). Accordingly there are several definitions of drought in common use (Wilhite and Glantz, 1985): meteorological drought (precipitation deficit), hydrological drought (low streamflow), agricultural drought (low soil moisture) and socioeconomic drought (including supply and demand). This complexity of droughts poses challenges for their attribution. It is not straightforward to disentangle these interacting factors, but over a long time period it may be possible that a signal can be detected.

Previous attribution studies for eastern Africa have mainly focussed on meteorological drought drivers (precipitation deficit), with recent studies finding little or no change in the risk of low-precipitation periods due to anthropogenic climate change (e.g., Philip et al., 2018a; Uhe et al., 2018). Some weather stations in eastern Africa have recorded a decrease in precipitation in recent years, however climate models generally project an increase in mean precipitation but give conflicting results for the probability of very dry rainy seasons (e.g. Shongwe et al., 2011). The reasons for the recent observed decrease in precipitation thus remains unclear, but the trend is within the large observed natural variability in the region, at least for the historical and current climate.

However, precipitation only covers one aspect of drought — that of the supply side of the water balance. The demand side is represented by actual evapotranspiration (ET), which is a function of moisture availability and evaporative demand. With increasing temperatures, there is an a priori assumption that rising evaporative demand will increase the demand side of the water balance and, all else equal, droughts will become more severe. However, this assumption is not based on analyses, which motivates an objective study.

In the current study we wish to align our drought definition as closely as possible with the major impact of drought — the threat to food security. Across eastern Africa, the quality and quantity of food production for domestic consumption is intimately linked to agricultural conditions. We therefore use the agricultural definition of drought — low soil moisture — because soil moisture is a better indicator of crop health than precipitation alone and embodies the net effect of the supply and demand side of the water balance, in regions without irrigation. Whilst short term single-season drought episodes can be severe, we choose to analyse changes in drought on annual rather than sub-annual time scales because the worst crises in food security in this region have occurred with multiple season droughts (Funk et al., 2015). We will also investigate the influence of the main meteorological drivers of soil moisture trends, i.e. precipitation and temperature.

Ideally, we would study the influence of temperature on soil moisture via evapotranspiration (ET), however observational records are very limited in time and space and as the spatial decorrelation lengths of evapotranspiration are short their informational value is limited. We therefore analyse evaporative demand, which is also referred to as "potential evapotranspiration" PET. PET is the amount of evaporation that would occur if an unlimited supply of water were available, which is calculable or available for both observations and model simulations and is a function of temperature, humidity, solar radiation and wind speed.

We investigate evaporative demand as a means to study the influence of temperature on soil moisture, however, for regions that are irrigated or where irrigation is being considered, evaporative demand itself can be regarded as more relevant than soil moisture as a measure of drought tendency.

Whilst attribution studies specifically for the east African region have not previously used soil moisture or PET to explore drought, PET has been used in various attribution or trend studies outside our region of study, to explore for example, the influence of climate change on the hydrological cycle in China (e.g. Yin et al., 2010; Li et al., 2014; Fan and Thomas, 2018), trends and variability at sites in West Africa Obada et al. (2017) and compound events of low precipitation and high PET in Europe Manning et al. (2018).

Summarizing, the objectives of this study are to (i) consider the attribution question "do increasing global temperatures contribute to drier soils and thus exacerbate the risk of agricultural drought (low soil moisture) in eastern Africa?" and (ii) to investigate if global-warming driven trends in precipitation or local temperature via PET explain any emerging trend in agricultural drought. Our approach to attribution comprises the following steps: (1) Definition of the study variables and explanation of the study regions, (2) Description of observational data and detection of trends in observations (3) Model evaluation including description of the models, (4) Attribution of trends in models, (5) Synthesis of the results. Assessments will be based on both observations and climate and hydrological model output on the annual time scale. We will illustrate the method using examples of recent droughts in eastern Africa.

The outline of the remainder of the paper is as follows: In Section 2 the chosen study regions are presented followed by a description of the datasets used in the study. In Section 3 we describe the stepwise approach to attribution used in this paper, including assumptions and decisions made and illustrative examples. In Section 4, the results are synthesized per region. Finally, the discussion and conclusions are presented in Sections 5 and 6.

2 Study variables, region and datasets

In this section, we present the chosen study variables and study regions in eastern Africa and the datasets used to provide the variables to be analysed. Brief descriptions of the projects from which the datasets originate are provided in the supplement.

2.1 Study variables and region

We analyse four different variables: soil moisture, precipitation, temperature, and PET. We average these variables over six regions, as trend analyses of time series of regionally averaged quantities are more robust than the same analyses for point locations. This is especially true for precipitation, which shows small-scale spatial variability if the time period is not long

Table 1. The six study regions. See also Fig. 1

Region	Long name	Latitude	Longitude	Seasonal precipitation peak(s)	Primary livelihood zone
WE	West Ethiopia	7°N-14°N	34°E-38°E	Aug	agropastoral/mixed land
EE	East Ethiopia	8°N-13°N	38°E-43°E	Apr, Jul/Aug	pastoral
NS	North Somalia/Somaliland region and East Ethiopia	5°N-12°N	43°E-52°E	Apr/May, Oct	pastoral
NK	North Kenya	2°N-4.5°N	34°E-41°E	Apr, Oct/Nov	pastoral
CK	Central Kenya	1.5°S-1.5°N	35°E-38.5°E	Apr, Nov	agropastoral/mixed land
SS	South Somalia	2°S-5°N	41°E-48°E	Apr/May, Oct/Nov	pastoral/agropastoral

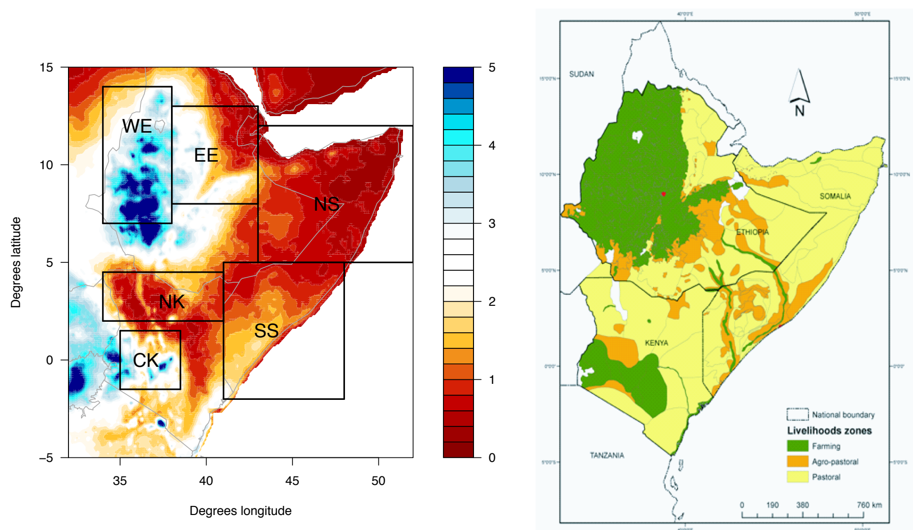

Figure 1. Left: annual mean precipitation [mm/day] and the six study regions. Note that only land values are used. Right: livelihood zones after Pricope et al. (2013), which were also used to define the study regions.

enough to sufficiently sample the distribution from multiple precipitation events. It is however necessary to select homogeneous zones, so that the signals present are not averaged out.

The focus of the study is on eastern Africa — Ethiopia, Kenya and Somalia (including the Somaliland region). We selected six regions based on precipitation zones, in which the annual mean precipitation and seasonal cycle are homogeneous (Fig. 1a), livelihood zones (see Fig. 1b) and discussions with local experts from Kenya Meteorological Department and the National Meteorological Agency (NMA) of Ethiopia and the Famine Early Warning Systems Network (FEWS NET). The regions are shown in Fig. 1 and listed in Table 1. Data is annually and spatially averaged over the study regions.

2.2 Datasets

For the four study variables, we use as many datasets as readily available over the study area, provided that (i) the data are sufficiently complete over a time period long enough to be used for trend calculations and (ii) the model data pass the validation tests (see Sect. 3). For this purpose, we decided to use time series of 35 years and longer. As the focus of this paper is on annual time scales, using monthly data is sufficient. The observational and model datasets used in this study are shown in Fig. 2 and listed in tables 2 and 3 below. For brief descriptions of the projects from which these data originate, please see the Supplement. Note that we use the data as it is available without applying any additional bias correction. Some of the data has undergone bias correction within project of origin, as described in the Supplement.

For observations of precipitation and daily mean near-surface temperature, we use gridded observational data sets and reanalyses.

For soil moisture and PET, no direct observations meeting the above criteria exist. Instead, we use observational estimates of soil moisture and PET resulting from various combinations of observational forcing data and models (see Fig. 2a).

Concerning soil moisture, observational series are few and generally too short to use for trend analysis and they do not correlate well with reanalysis or model data over eastern Africa (McNally et al., 2016). It is therefore important to use multiple observationally forced model estimates to span the large uncertainties from inter-dataset differences. There being no a priori reason to favour one soil moisture dataset over another, we treat all resulting soil moisture datasets equally. For all soil moisture data sets, observed and modelled, we use the topmost layer (see Fig. 2 for the depth of the topmost layer) provided by each dataset and scale each time series to have a standard deviation of 1 in order to make comparisons in trends possible. An exception to this is weather@home where the available soil moisture variable is an integrated measure of all four layers of soil moisture in the model, including the deep soil.

PET is a function of temperature, humidity, solar radiation and wind speed, and as such is not a directly observable variable. Observational estimates of PET used here originate from reanalysis data sets or reanalysis-driven impact models. For both observed and modelled PET, there are various ways of parametrizing PET, ranging from simple temperature or radiation-based schemes to sophisticated schemes based on all the aforementioned components. Whilst the Penman-Monteith scheme is often considered superior (e.g. Hobbins et al., 2016), one is often constrained from using a Penman-Monteith parameterization due either to the lack of accurate or reliable input data or because the choice of PET parameterization within a given hydrological model setting is already prescribed, as in the ISIMIP ensemble. We thus chose to use a variety of PET parameterizations and input datasets in order to cover the range of possible PET values and trends in PET. The PET scheme used by each data set is noted in Fig. 2.

Concerning model data sets, most simulations stem from the ISIMIP project, which provides output of the variables under investigation for four different impact models driven by four different GCMs. These simulations are complemented by other readily available model runs with different (but compatible) framings.

With the datasets we use we cover a wide range of different factors that influence PET and soil moisture. The different factors include meteorological forcing, model choice, RCP scenario for the greenhouse gas concentration trajectory, PET

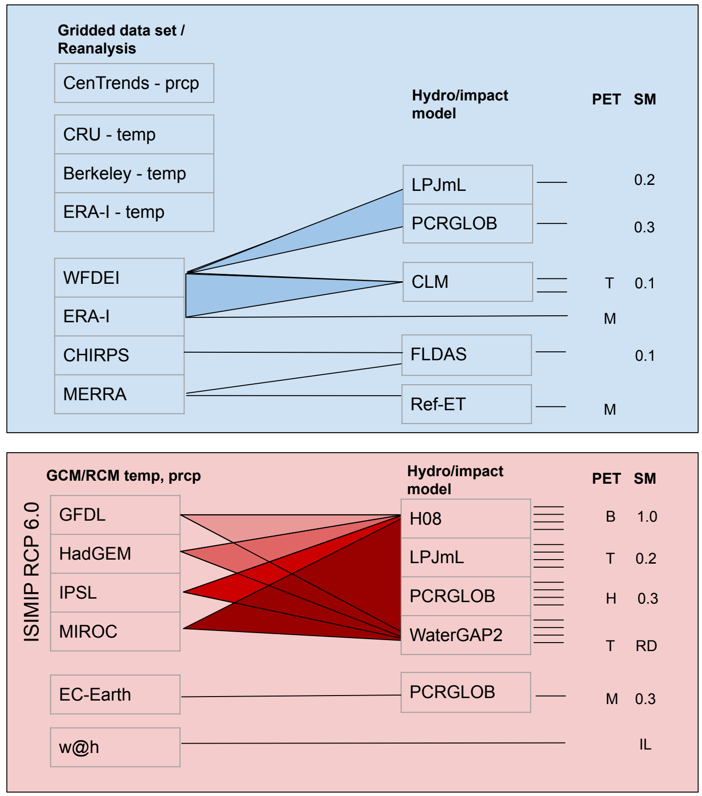

Figure 2. Datasets used in this paper. Top: observational precipitation (prcp) and near-surface temperature (temp) datasets, bottom: models. Listed under PET is the PET scheme (T: Priestley-Taylor, M: Penman-Monteith, H: Hamon, B: Bulk formula) and, under SM, is the depth of the top soil moisture layer available (RD: depends on rooting depth (0.1-1.5m for WaterGAP2); IL: integrated over all layers). Shading indicates an experiment with either multiple input datasets or multiple hydrological models. The number of resulting hydrological model simulations are indicated by horizontal lines on the right side of the figure.

scheme, number of soil layers and depth of topsoil layer, dynamic vegetation modelling (LPJmL only) and transient versus time slice runs (see next section on ‘Methods’).

3 Methods

In this section we describe first the method we use for detection and attribution of trends in the four variables, including model validation and the synthesis of observational and model results. Furthermore, in subsection 3.2 we describe the assumptions

Table 2. Observational data used in this study.

Observational dataset	Full name	Time period used	Spatial resolution (°lat x °lon)	Reference(s)
Observatational/reanalysis data set				
CenTrends (prcp)	Centennial Trends data set	1900–2014	0.1x0.1	Funk et al. (2015)
CRU TS4 (temp)	CRU TS4.01	1901–2019	0.5x0.5	Harris et al. (2014)
Berkeley (temp)	Berkeley Earth	1750–2019	1.0x1.0	Rohde et al. (2013b, a)
ERA-I	ERA-Interim	1979–2019	0.5x0.5	Dee et al. (2011)
Observation-driven hydro/impact model				
LPJmL-WFDEI (soil moisture)	Lund-Potsdam-Jena managed Land - WATCH-Forcing-Data-ERA-Interim	1971–2010	0.5 x 0.5	Bondeau et al. (2007); Rost et al. (2008); Schaphoff et al. (2013); Weedon et al. (2014)
PCRGLOB-WFDEI (soil moisture)	PCRaster GLOBal Water Balance model - WATCH-Forcing-Data-ERA-Interim	1971–2010	0.5 x 0.5	Sutanudjaja et al. (2018); Weedon et al. (2014)
CLM-ERA-I (soil moisture, PET)	Community Land Model version 4 - ERA-Interim	1979–2016	0.5 x 0.5	Oleson et al. (2010)
CLM-WFDEI (soil moisture, PET)	Community Land Model version 4 - WATCH-Forcing-Data-ERA-Interim	1979–2013	0.5 x 0.5	Lawrence et al. (2011); Weedon et al. (2014)
FLDAS (soil moisture)	Famine Early Warning Systems Network (FEWS NET) Land Data Assimilation System	1981–2018	0.1 x 0.1	McNally et al. (2017)
MERRA Ref-ET (PET)	Modern-Era Retrospective analysis for Research and Applications Reference Evapotranspiration	1980–2018	0.125 x 0.125	Hobbins et al. (2018)

Table 3. Model data used in this study.

Model dataset	Full name	Time period used	Spatial resolution (°lat x °lon)	Reference(s)
GCM/RCM				
GFDL	GFDL-ESM2M, Geophysical Fluid Dynamics Laboratory - Earth System Model 2M	1861–2018	2.02x2.5	Dunne et al. (2012, 2013)
HadGEM	HadGEM2-ES, Hadley Centre Global Environmental Model version 2-ES	1859–2018	1.25x1.88	Collins et al. (2011); Jones et al. (2011)
IPSL	IPSL-CM5A-LR, Institut Pierre Simon Laplace - CM5A-LR	1850–2018	1.89x3.75	Dufresne et al. (2013)
MIROC	MIROC5, Model for Interdisciplinary Research on Climate - version 5	1850–2018	1.4x1.4	Watanabe et al. (2010)
EC-Earth	EC-Earth 2.3	1850–2018	1.12x1.125	Hazeleger et al. (2012)
w@h (temp, prcp, soil moisture)	Weather@home	2005–2016 and counterfactual climate	0.11x0.11	Massey et al. (2015); Guillod et al. (2017)
Hydro/impact models				
H08 (soil moisture, PET)	H08	1861–2018	0.5x0.5	Hanasaki et al. (2008a, b)
LPJmL (soil moisture, PET)	Lund-Potsdam-Jena managed Land model	1861–2018	0.5x0.5	Bondeau et al. (2007); Rost et al. (2008); Schaphoff et al. (2013)
PCRGLOB (soil moisture, PET)	PCRGLOB-WB, PCRaster GLOBal Water Balance model	1861–2018	0.5x0.5	Sutanudjaja et al. (2018)
WaterGAP2 (soil moisture, PET)	Water Global Analysis and Progress Model version 2	1861–2018	0.5x0.5	Müller Schmied et al. (2016)

and decisions that are made concerning the data/model setup and in subsection 3.3 we provide an example of how the method is applied to real data.

3.1 Detection and attribution of trends

We use a multi-method, multi-model approach to address attribution. We use global mean surface temperature (GMST) as a measure for anthropogenic climate change for calculating trends. We calculate trends for all variables, regions and datasets and synthesize results into one overarching attribution statement for each of the four variables in each of the six regions. We use this method, following the approach applied in earlier studies on drought in eastern Africa (e.g., Philip et al., 2018a; Uhe et al., 2018) and other drought- and heat-attribution studies (e.g., Philip et al., 2018b; van Oldenborgh et al., 2018; Kew et al., 2019; Sippel et al., 2016), which represents the current state of the art in extreme event attribution. The method is extensively explained in van Oldenborgh et al. (2019), Philip et al. (2019), van Oldenborgh et al. (2018) and van der Wiel et al. (2017).

In this study, for transient model runs and observational time series, we statistically model (i.e., fit) the dependency of annual means of the different variables on GMST, (the model GMST for models, and GISTEMP surface temperature GMST (Hansen et al., 2010) for observations and reanalyses) as follows:

After inspection of whether a Gaussian or a General Pareto Distribution fits the observational or reanalysis data best, we use the following distributions:

- for soil moisture: a Gaussian distribution that scales with GMST, focussing on low values,
- for precipitation: a General Pareto Distribution (GPD) that scales to GMST, analyzing low extremes
- for temperature: a Gaussian distribution that shifts with GMST, focussing on high values, and
- for PET: a Gaussian distribution that scales with GMST, focussing on high values.

When the distribution is shifted, a linear trend α is fitted by making the location parameter μ dependent on GMST as

$$\mu = \mu_0 + \alpha T, \tag{1}$$

with α in [units of the study variable]/K. When the distribution is scaled,

$$\mu = \mu_0 \exp(\alpha T/\mu_0), \tag{2}$$

$$\sigma = \sigma_0 \exp(\alpha T/\mu_0), \tag{3}$$

which keeps the ratio of the location and scale parameter σ/μ invariant. In each case, the fitted distribution is evaluated twice: once for the year 1900 and once for the year 2018. Confidence intervals (CI) are estimated using a non-parametric bootstrapping procedure. This allows us to calculate the return period of an event as if it would have happened in the year 1900 or in the year 2018. To obtain a first-order approximation of the percentage change between the two reference years, α is multiplied by 100% times the change in GMST and divided by μ_0 (for the shift fit this is exact). Note that for some variables — e.g., precipitation — it is appropriate to scale rather than shift the distribution with GMST (see van Oldenborgh et al., 2019; Philip et al., 2019, for an explanation). For the very large weather@home ensemble simulations of actual and counterfactual climates, it is not necessary to use a fitting routine as the large amount of data permits a direct estimation of the trend. This also provides an opportunity to check the assumptions made in the fitting, notably that the values follow an extreme-value distribution and that the distribution shifts or scales with the smoothed GMST. We calculate trends for the time series of spatially and annually averaged data of all four variables and all six regions for all datasets by dividing the difference in the variable between the two ensembles by the difference in GMST.

Figures 3 and 4 present the methods applied to transient series and time slices respectively. For reference and to aid interpretation of the return-period diagrams, the magnitude of a hypothetical event with a 20-year return period in the year 2018 or in the current climate is shown as a horizontal line or square. Reading the return period at which this line crosses the fit for the reference year 1900 shows how frequent an event with a 20-year return period in today's climate would have been then.

We only use results from model runs if they pass two different validation tests — a qualitative test on the seasonal cycle and a stronger test on variability. For soil moisture, due to the difficulties in obtaining reliable soil moisture measurements (e.g., Liu and Mishra, 2017) and the differences between the observational (reanalysis) datasets, we cannot assume that observational or reanalysis data are more accurate than model data. Therefore we simply use the soil moisture model data if the model input — PET and precipitation — passed the validation tests.

We perform only a qualitative validation of the seasonal cycle. For each region, each variable, and each model we check that the seasonal cycle resembles that of at least one of the observational datasets, in both the number and the timing of peaks. If the seasonal cycle is very different, we do not use the time series for that specific combination. This is the case for the original GCM precipitation in region NK for weather@home and in regions NK and CK for MIROC (the seasonal cycle is improved in the adjusted dataset, so we still use the time series in soil moisture) and for temperature in region SS for EC-Earth (we do not have adjusted data to check so we do not use this model-region combination for soil moisture or PET).

The second validation test is on the model variability in precipitation and PET (variability relative to the mean for variables that scale with GMST). If the model variability of a specific variable in a specific region is outside the range of variability calculated from observations or reanalyses, we do not use that specific dataset for that specific region and variable. For temperature, we relax the validation criteria on variability as it became clear during the analysis that the trend in soil moisture does not depend strongly on temperature and the trend in temperature agrees between models and observations. In two of the regions a strict validation resulted in only two driving GCMs. Trends from the resulting time series that passed the validation tests are shown in Section 4 and in the figures in the Supplementary Information.

Using the large weather@home ensemble (which requires no fitting), we check the assumption that precipitation and soil moisture scale with GMST and temperature shifts with GMST. For PET, we assume that the distribution scales with GMST. In the weather@home ensemble, dry extremes show less change than intermediate dry extremes, which supports our assumption that scaling with GMST is appropriate (except for the higher return values, where the uncertainties are large). For soil moisture it is very difficult to distinguish between scaling and shifting from the weather@home ensemble because the trend is small. For temperature the weather@home ensembles indicate that the highest temperatures are increasing slower than the lower temperatures. This implies that the variability decreases with GMST, however no consistent signal in the observations or other

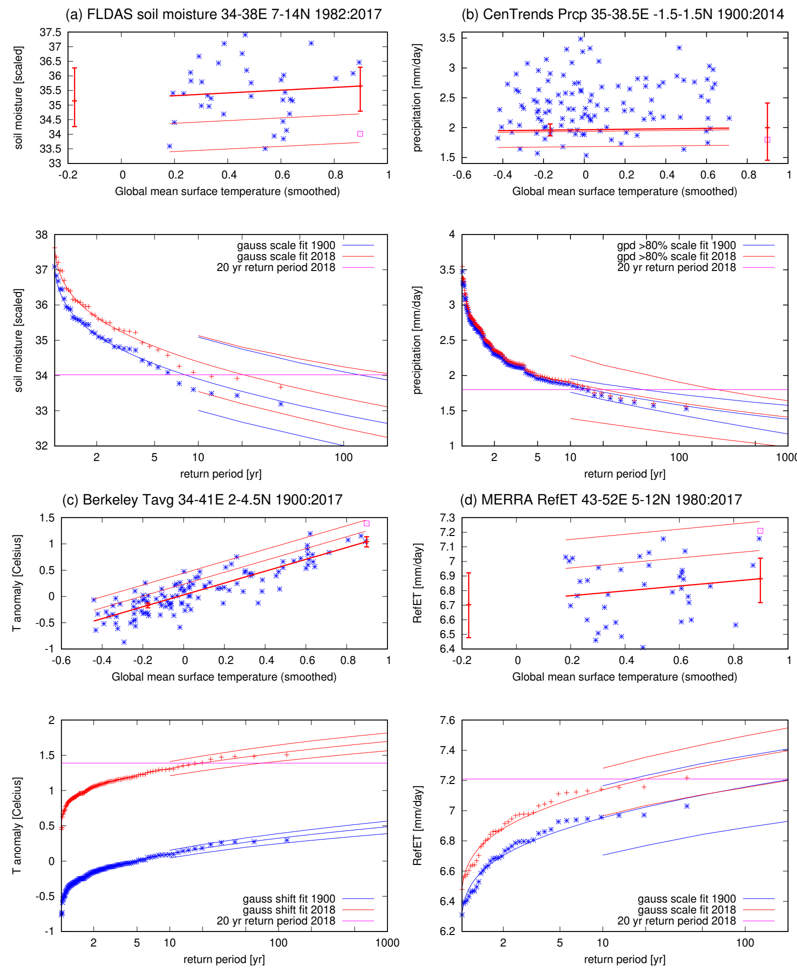

Figure 3. Illustrative examples of the fitting method for each variable, for selected study regions. (a) FLDAS soil moisture (Gauss fit, low extremes, region WE); (b) CenTrends precipitation (GPD fit, low extremes, region CK); (c) Berkeley temperature anomaly (Gauss fit, high extremes, region NK); (d) MERRA PET (Gauss fit, high extremes, region NS). Top of each panel: annually averaged data (stars) against GMST and fit lines - the location parameter μ (thick), $\mu{\pm}\sigma$ and $\mu \pm 2\sigma$ (thin lines, Gaussian fits) and the 6 and 40 year return values (thin lines, GPD fit). Vertical bars indicate the 95% confidence interval on the location parameter μ at the two reference years 2018 and 1900. The magenta square illustrates the magnitude of an event constructed to have a 20-year return period in 2018 (not included in the fit). Bottom of each panel: return period diagrams for the fitted distribution and 95% confidence intervals, for reference years 2018 (red lines) and 1900 (blue lines). The annually averaged data is plotted twice, shifted or scaled with smoothed global mean temperature up to 2018 and down to 1900. The magenta line illustrates the magnitude of a hypothetical event with a 20-year return period in 2018.

models is evident (we see a small increase in variability with time for Berkeley, a small decrease for CRU and no consistency between the models). This does not affect the trend much, which is evaluated for the centre of the distribution.

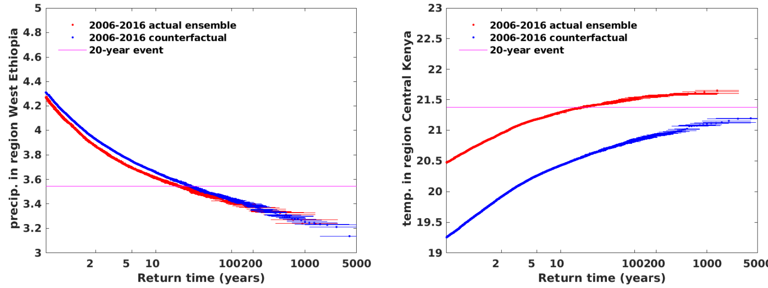

Figure 4. Illustrative examples of the weather@home time slice model runs. Left: annual mean precipitation in region WK. Right: annual mean temperature in region CK. The red markers are for the present day climate and the blue markers are for the climate in pre-industrial times. The magenta line illustrates the magnitude of a hypothetical event with a 20-year return period in the present day climate.

Trends are presented as change in a variable per degree of GMST warming. We show trends rather than probability ratios, which conveniently results in finite ranges in confidence intervals for all variables. This is not the case for the probability ratio, where, for example, strong trends in temperature imply that mild extremes of the 2018 climate (e.g., a 1-in-20-year event) would have had a chance of almost zero around 1900, resulting in very large probability ratios and extensive extrapolation of the fit beyond the length of the dataset.

We synthesize the trends of all data that passes the validation tests in the following manner, see also Fig. 5. The observational (reanalysis) estimates are based on the same natural variability: the historical weather. They also cover similar time periods. The uncertainties due to natural variability (denoted as solid blue in the synthesis figures) are therefore highly correlated. We approximate these correlations by assuming the natural variability to be completely correlated, and compute the mean and uncertainties as the average of the different observational estimates. The spread of the estimates is a measure of the representation uncertainty in the observational estimate and is added as an independent uncertainty to the natural variability (black outline boxes). This results in a consolidated value for the observations (reanalyses) drawn in dark blue.

In contrast, model estimates have more uncorrelated natural variability: totally uncorrelated for coupled models; and largely uncorrelated for SST-forced models (the predictability of annual mean precipitation given perfect SSTs is low in eastern Africa). We approximate these correlations by taking the natural variability to be uncorrelated. The spread of model results can be compared by the spread expected by the natural variability by computing the χ^2/dof statistic. If this is greater than one, there is a noticeable model spread, which is added in quadrature to the natural variability. This is denoted by the white boxes in Fig. 5. The bright red bar indicates the total uncertainty of the models, consisting of a weighted mean using the (uncorrelated) uncertainties due to natural variability plus an independent common model spread added to the uncertainty in the weighted mean.

Finally, observations and models are combined into a single result in two ways. Firstly, we neglect model uncertainties beyond the model spread and compute the weighted average of models and observations: this is indicated by the magenta bar. However, we know that models in general struggle to represent the climate of eastern Africa, so the model uncertainty is larger than the model spread. Therefore, secondly, we use the more conservative estimate of an unweighted average of observations and models, indicated by the white box around the magenta bar. This gives more weight to the observations.

3.2 Assumptions and decisions

We made the following assumptions and decisions about the data and model set-up in addition to completing the model evaluation to attain data of sufficient quality.

1. As was shown by Funk et al. (2015), the CenTrends precipitation dataset includes many different sources of precipitation data and more stations than most other datasets. We therefore assume for precipitation that the CenTrends dataset is superior to other datasets over our region of study. We therefore only use the CenTrends dataset for observations of precipitation.

2. In general we use the longest time series of data available. We make exceptions in the starting year if necessary, based on visual inspection of abrupt changes due to data limitations toward the beginning of the time series.

   (a) We use Berkeley from 1900 and in region SS from 1920.

   (b) We use CRU starting from 1940 instead of 1901 in regions NK, CK and SS.

3. We do not know of a realistic soil moisture dataset that covers a long-enough time period to calculate trends. Therefore we do not select simulations based on evaluation criteria other than selecting runs based on PET and precipitation evaluation in the input variables.

4. As models do not share a consistent set of soil moisture levels, we take the top level of each model, assuming that this is the most comparable level across models. We checked for LPJmL — the only selected ISIMIP hydrological model that has more than one level available for soil moisture — that the variability does not change by much when integrating over multiple levels instead of using level 1.

5. Within the ISIMIP project, variables required by the hydrological models, including temperature and precipitation, were bias corrected and the adjusted data was used to calculate PET and to drive the hydrological models to output soil moisture. In the synthesis, however, we present results for temperature and precipitation based on the unadjusted data, on principle that this better spans the range of model uncertainty in temperature and precipitation. The bias correction applied in ISIMIP aims to conserve the original trend. In accordance, we find little change in trend for most time series, see Section 5.

6. Instead of PET, RefET(reference evapotranspiration) was available for the MERRA dataset. RefET can be converted to potential evapotranspiration by multiplying its value to a reference crop coefficient. We assume using RefET instead of PET does not influence the overall conclusions and we do not convert RefET into PET.

7. We focus on the historical time-frame. Therefore the trends in different RCP and socio-economic scenarios will be relatively similar to each other. The forcing data is the same for the years 1860–2005 and only differs for the most recent years, from 2006 onwards. In general, however, using different scenarios can be seen as an advantage, as a greater range of scenario uncertainty will be spanned.

   (a) We use RCP6.0 in ISIMIP as this choice resulted in the largest number of simulations and RCP8.5 in EC-Earth as this was the only scenario available.

   (b) The socio-economic scenario selected in ISIMIP model runs is *historical*, for 1860–2005 and *2005soc* for 2006–present, except for H08 for which *historical* was not available for years 1860–2005 and we instead use *2005soc* for those years as well as years 2006–present. For the WFDEI experiments, *2005soc* was not available. Instead we use *varsoc* for the years 2006–2018 and *historical* before 2006.

8. Trends are calculated or extrapolated using all data up to 2018 and between the pre-industrial era (1900) and the present (2018). Weather@home is an exception where trends are calculated between two stationary climates of the present and the pre-industrial era. Differences in trends can arise due to different time periods and lengths of datasets, which are generally shorter for observations and reanalyses than for model simulations. However, we consider the use of all available observational and reanalysis data and different model framings to lead to a more complete and robust attribution statement.

9. We analyse Jan–Dec annual means. Based on the seasonal cycles of precipitation and temperature, for all regions except for region WE (which has a single rainy season) we could also have chosen to analyse Jul–Jun annual means instead. The influence of this choice on the trends is low (see also Sect. 3.3).

10. For consistency in the method, we fit the variability as a constant over time for all data. In both observed time series and simulations we see very little or no trend in variability up to 2018.

11. If for observational data a Gaussian fit is the best fit, we also fit model data to a Gaussian, even if a GPD is a better fit for that data. In doing this we avoid erroneous comparisons between the variable mean and variable extreme. We checked for model runs in which this disparity occurs, but found that in most cases the trend calculated from fitting model data to a GPD was not very different from the trend calculated from fitting model data to a Gaussian.

3.3 Illustrative examples

In this section we show an example to illustrate the method of detection of trends in precipitation data, as people often initially experience droughts as reduced or failed rainy seasons. For this purpose, we calculated return periods and risk ratios of recent droughts defined as low-precipitation events on the annual time scale, see Table 4. Note that the risk ratios are calculated from CenTrends alone and are not synthesized values based on a multi-model analysis. The synthesis of observations with models follows in the next section. We choose events based on the Emergency Events Database (EM-DAT) — an extensive global database of the occurrence and effects incurred from extreme weather events, and the time series calculated from CenTrends (up to December 2014 only, which excludes the recent droughts of 2015 and 2016/2017). For the northern three study regions we choose the year 2009, in which the first rainy season failed (in region WE, where there is only one peak in precipitation, the whole season had slightly lower precipitation amounts). For the southern three study regions we choose the year 2005, in which the second rainy season failed. Additionally, we also investigate the well-known 2010/2011 drought for the regions NK and SS. As this drought occurred over the latter part of 2010 and the first part of 2011 (the second part of 2011 was in fact very wet), we define the annual period of this specific 2010/2011 analysis to be Jul–Jun.

The results show, for instance for region WE, that in CenTrends the trend in precipitation between 1900 and 2018 is -0.09 mm/day/K (95% confidence interval (CI) -0.51 to 0.14 mm/day/K). With a change in GMST of 1.07 K and a mean precipitation in 1900 of 3.2 mm/day this is similar to a change of 3%. This means that if an event with the same precipitation amount as in the year 2009 had happened again in 2018 it would have been a one in 30 (95% CI 2 to 400) year event in 2018, whereas in 1900 it would have been a one in 80 (95% CI 30 to 1400) year event, corresponding to a probability ratio of 2.5 (95% CI 0.2 to 380). A return period that decreases in time indicates that such extreme droughts are becoming slightly more common, however, in this example we see large uncertainties consistent with no change. Note that the trend and probability ratio are not significantly different from zero at $p < 0.05$. The results for all regions are summarized in Table 4. We note that the trends calculated for the Jan–Dec events and for the Jul–Jun events in regions NK and SS respectively are not significantly different. This supports the decision to analyze Jan–Dec annual extremes only.

4 Synthesis results

In this section, to illustrate the synthesis method, intermediate synthesis figures, which not only show the overall synthesis but also the results for individual models, are presented for the region SS for each of the four variables. See the caption of Fig. 5 for more information. The intermediate synthesis figures of all six regions can be found in the Supplementary Information. Table 5 and Fig. 6 summarize all final synthesized findings. Using both the intermediate and final synthesis results we first draw conclusions based on different GCMs and hydrological models and then turn to conclusions per variable.

First we look for consistent behaviour in the trends from individual GCMs across the four variables. Some general conclusions about the different GCMs are as follows: (i) for GCM-driven model runs with stronger positive trends in temperature, there is a tendency that the positive trends in PET are also stronger and vice versa; (ii) the uncertainty in precipitation trends is high compared to the trend magnitudes. This is one of the reasons why a clear relation with soil moisture trends is not evident; (iii) no clear relation between local temperature trends and soil moisture trends is evident.

Looking at the different hydrological models we conclude that the trend in PCR-GLOBWB PET, which uses the Hamon PET scheme that depends only on temperature, is generally higher than the trend in in EC-Earth PET, which uses the more-complex Penman-Monteith PET scheme that additionally depends on humidity, wind and radiation. Using this more complex scheme can influence the trend in soil moisture, especially in wetter regions.

Table 4. Trends, return periods and probability ratios of equivalent events in the year 2018 and 1900 for three recent drought events registered in the EM-dat database (2005, 2009 and 2010/2011), based on annual average precipitation (mm/day) from the CenTrends dataset. 95 % confidence intervals are given between brackets. For each study region impacted by the events, the annual precipitation for the event year ($Prcp$, used to define the event magnitude) and the 1900–2014 climatological precipitation average ($\overline{ClimPrcp}$) is given. The asterisk (*) denotes that Jul–Jun is taken instead of Jan–Dec to define a year.

Region	**Event year**	$Prcp$	$\overline{ClimPrcp}$ **1900-2014**	**Trend [mm/dy/K]**	**Return period in 2018**	**Return period in 1900**	**Probability ratio**
WE	2009	2.94	3.38	-0.09 (-0.51 to 0.14)	30 (2 to 400)	80 (30 to 1400)	2.5 (0.2 to 380)
EE	2009	1.49	1.84	-0.03 (-0.35 to 0.07)	40 (3 to 340)	50 (25 to 560)	1.4 (0.4 to 70)
NS	2009	0.42	0.63	0.07 (-0.08 to 0.12)	80 (4 to 300)	10 (5 to 46)	0.13 (0.03 to 6.7)
NK	2005	0.77	1.10	-0.07 (-0.26 to 0.12)	5 (2 to 30)	10 (5 to 22)	1.9 (0.3 to 6.5)
CK	2005	1.75	2.39	0.04 (-0.55 to 0.43)	29 (3 to 200)	22 (12 to 63)	0.77 (0.11 to 14)
SS	2005	0.74	1.09	0.03 (-0.12 to 0.22)	29 (4 to 470)	17 (6 to 47)	0.61 (0.02 to 7.80)
WK	2010/ 2011*	0.51	1.10	0.16 (-0.30 to 0.27)	650 (10 to 20000)	130 (53 to 2200)	0.21 (0.03 to 64)
SS	2010/ 2011*	0.53	1.09	0.02 (-0.31 to 0.21)	300 (12 to 40000)	230 (90 to 8100)	0.77 (0.03 to 80)

Table 5. Summary of synthesis results for each region and study variable. Note that '0' means no *significant* change and a '+' sign indicates a positive trend, where in soil moisture this means a change towards a *wetter* soil. The uncertainties associated with each result are depicted in Fig. 6

Region	**Soil moisture**	**Precipitation**	**Temperature**	**PET**
WE	0/+	0/+	+	+
EE	0	0	+	+
NS	0/+	+	+	+
NK	0/+	0/+	+	0/+
CK	0/+	0	+	0/+
SS	0/+	0/-	+	+

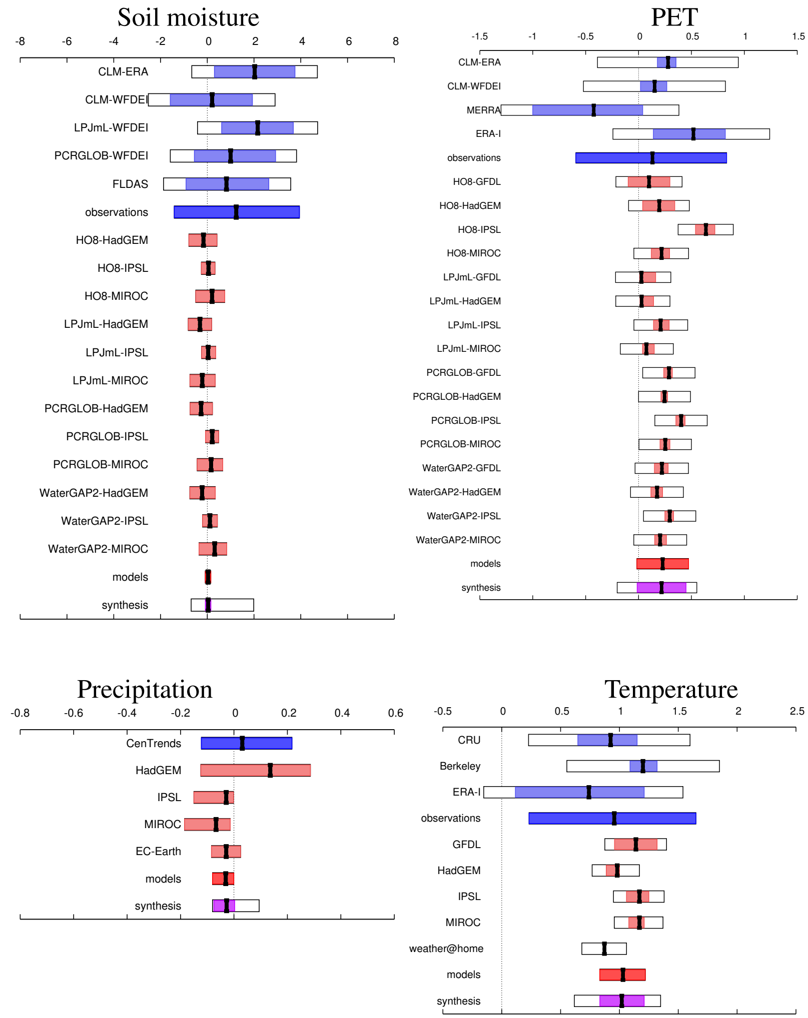

Figure 5. Illustrative examples of the synthesized values of trends per degree GMST rise for soil moisture (top left), PET (top right), precipitation (bottom left) and temperature (bottom right) for region SS. Black bars are the average trends, colored boxes denote the 95% CI. Blue represents observations and reanalyses, red represents models and magenta the weighted synthesis. Coloured bars denote natural variability, white boxes also take representativity / model errors into account if applicable (see Sect. 3). In the synthesis, the magenta bar denotes the weighted average of observations and models and the white box denotes the unweighted average. Soil moisture trends are based on standardized data, the other trends are absolute trends.

The analyses of the individual model runs, stratifying by GCM or hydrological model, do not lead to a clear conclusion on the relation between the trends in precipitation, temperature, PET and soil moisture. We therefore turn to the analysis of the synthesized values, see Table 5 and Fig. 6 for a summary of the outcome and Fig. 5 and Figs. S1 to S6 in the Supplementary Information for synthesis diagrams. The table gives a concluding interpretation of the synthesized results shown in Fig. 6.

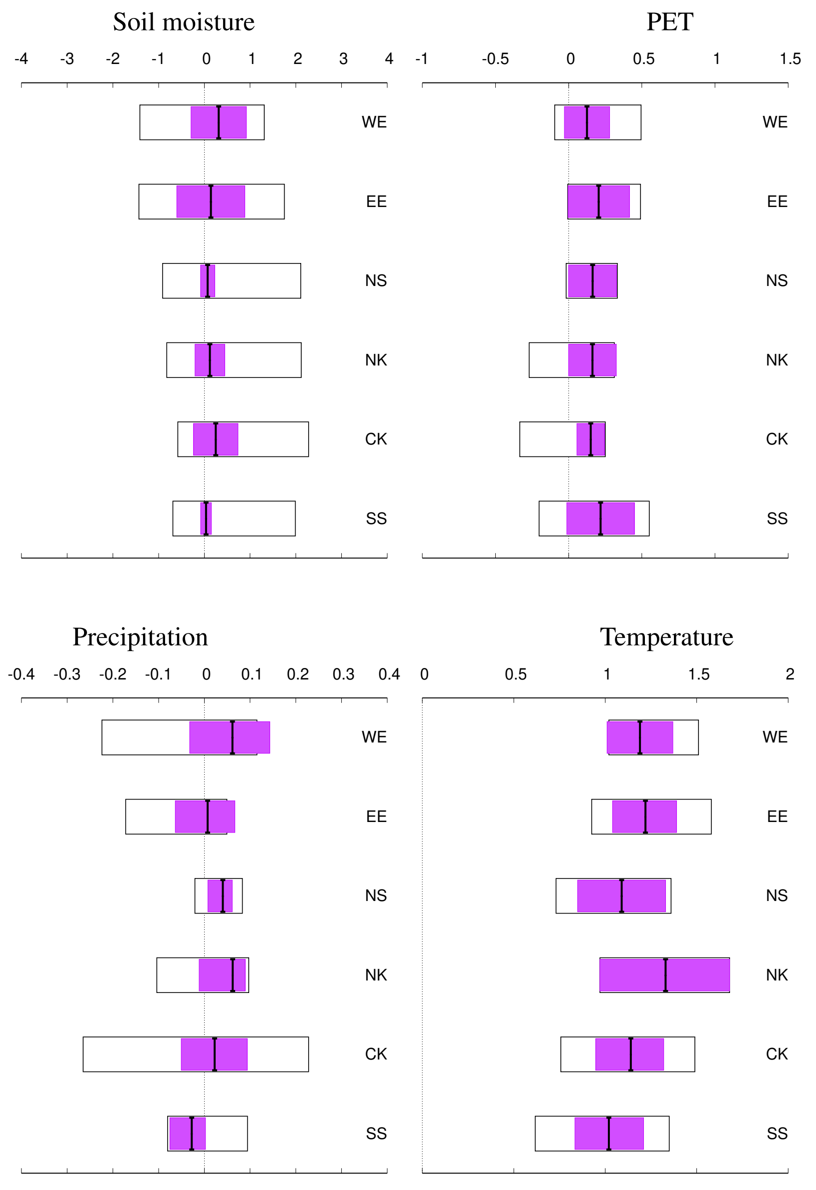

Figure 6. Summary of the synthesized values for soil moisture, PET, precipitation and temperature in the six regions. The magenta bars denote the weighted averages of observations and models and the white boxes denote the unweighted averages.

For soil moisture we find no significant synthesized trends: there is practically no change in region EE and no trend to a small positive non-significant trend in regions WE, NS, NK, CK and SS.

For precipitation, regions WE and NK show a positive but non-significant trend, in region NS there is a small positive trend, regions EE and CK show no trend and region SS a negative non-significant trend.

As expected from global climate change, the local annually averaged temperatures all have a significant positive trend, with best estimates between 1.0°and 1.3°per degree of GMST increase. Related to this, trends in PET are also positive in four of the six regions but lower than for temperature and generally with larger confidence intervals. The regions NK and CK are the exceptions. Although weighted averages show positive trends, models show tendencies opposite to observations. This incompatibility renders the results uncertain.

We can identify the following relationships between different variables: (i) Precipitation trends have a (small) influence on soil moisture trends in regions WE, NS and NK; (ii) in regions WE, EE, NS, NK and CK, temperature and PET have no discernible influence on soil moisture trends; (iii) in region SS, the non-significant negative trend in precipitation does not lead to lower soil moisture and neither do the trends in temperature or PET.

5 Discussion

In this section, we discuss the interpretation of our results in the light of how choices and assumptions made may have influenced the outcome and we compare previous studies on similar topics.

We study drought trends on annual as opposed to sub-annual time scales, as long-term drought presents a greater risk for food security. We define the annual period to be from January to December. This definition is a natural choice for each of our study regions, where the single or dual seasonal cycle peaks in precipitation (rainy seasons) and temperature do not extend beyond December into the next year. The Jan–Dec definition has the consequence that multi-season droughts out of phase with this period do not appear extreme in the observational time series used here, whilst they would appear extreme in a Jul–Jun series. For example, in the well-documented 2010/2011 drought event in eastern Africa, only the second rainy season in 2010 and first rainy season of 2011 were exceptionally dry. This choice however does not affect the resulting annual trends, which are similar for both the Jan–Dec and Jul–Jun annual definition.

On the annual time scale, we do not see strong explanatory relationships between the *trends* in the four studied variables. To gain insight in the relationships between the variables, we additionally looked at correlations on a sub-annual time scale. Simple correlations between monthly precipitation, temperature, PET and soil moisture (not shown) support the conclusions of Manning et al. (2018) on the influence of precipitation and PET on soil moisture at dry sites in Europe. They found that at water-limited sites the influence of precipitation on soil moisture is much larger than the influence of temperature, via PET, on soil moisture. In our study, we find the same for the driest regions and the driest months in the wetter regions, and for the more temperature-based PET schemes.

Looking at seasonal cycles — monthly means averaged over recent decades — a comparison between seasonal cycles of the different variables shows that the seasonal cycle of soil moisture is similar to that of precipitation in all six study regions. In contrast, the inverse seasonal cycle of temperature is not similar to that of soil moisture. Whether the PET seasonal cycle reflects elements of the soil moisture cycle or not depends on the PET scheme used: temperature- or radiation-based schemes show a seasonal cycle that is similar to that of temperature, whereas more advanced schemes reflect a mixture between the seasonal cycles of precipitation and temperature.

We thus conclude that the influence of precipitation on soil moisture is higher than that of temperature or PET. This is supported by the synthesized results that show negligible or no trends in soil moisture and precipitation whereas the trends in temperature and PET are strongly positive.

If temperature has, via PET, an influence on trends in soil moisture, we expect to see that the positive trend in temperature is coupled to a drying trend in soil moisture. As we average over the annual scale, we may miss parts of the season when this effect is strongest. Therefore we selected a region and period outside the rainy season, in which the seasonal peak in temperature corresponds to a dip in soil moisture (region CK, months Feb–Mar), to inspect sub-annual trends (not shown). Even then, we find that there is no negative trend in soil moisture accompanying the positive temperature trends.

While improving the data with respect to some characteristics, an additional uncertainty arises from the bias correction of the GCM data prior to use in the hydrological model. The bias correction in ISIMIP was set up to preserve the long-term trend, but it also decreases the daily variability by truncating extreme high values (e.g., in precipitation) (Hempel et al., 2013). The most important element for our analysis is that it also increases the daily variability by removing excessive drizzle, which is often present in GCM precipitation data. Prudhomme et al. (2014) noted that such a statistical bias correction can influence the signal of runoff changes but that the effect generally remains smaller than the uncertainty from GCMs and global impact models. By far the largest difference we found in our analysis between trends in original and bias-corrected data was for temperature for IPSL in region NK: we found 1.9 K/K (95% CI 1.8 to 2.1 K/K) for the original trend and 1.4 K/K (95% CI 1.3 to 1.5 K/K) for the trend in bias-corrected data. All other differences were smaller and non-significant.

A study by Rowell et al. (2015) discussed the possibility that climate model precipitation trends in East Africa are influenced by inability of the models to represent key physical processes reliably. In attribution studies on drought, especially for this region, it is therefore high priority to extend model evaluation techniques to assess models' representation of key physical processes. The approach taken in this paper has been to apply simple evaluation techniques on the seasonal cycle and frequency distributions of readily available data and that results from models passing validation tests represent the status of our current knowledge. Rainy seasons in this region are governed by large-scale processes, such as the shifting of the ITCZ and ENSO dynamics. The ability of a model to capture the seasonal cycle in precipitation and temperature thus provides some assurance that large-scale physical processes are reasonably well described by the model. We see the tests we perform as a minimum requirement for model validation. However, to improve the performance of models and to understand the discrepancies between models and observations, a much more thorough investigation into the models' representation of physical processes and feedbacks is required, such as demonstrated by James et al. (2018) and encouraged by the IMPALA (Improving Model Processes for African Climate) project (https://futureclimateafrica.org/project/impala/).

It is still unknown how vegetation will respond to substantial increases of CO_2 concentration. Two counteracting effects — physiological (restriction of stomatal openings leading to decreased evapotranspiration) and structural (increased leaf area leading to more stomata and increased evapotranspiration) responses — are expected, but their net effect is unknown (e.g. Wada et al., 2013). So-called 'dynamic vegetation models' include these CO_2 effects and there are indications that these models show a weaker response of drought to climate change (Wada et al., 2013; Prudhomme et al., 2014). In this study our selection of hydrological models is restricted by the variables we require, however, out of the four ISIMIP hydrological models that match our criteria, one (LPJmL) uses dynamic vegetation modeling. The soil moisture response to increasing GMST in LPJmL simulations is mid-range amongst the ISIMIP results. The PET response for LPJmL simulations is, however, somewhat on the low side of the ISIMIP results. It has not been verified if this behaviour is linked to dynamic vegetation modelling, but with confidence intervals generally overlapping with the synthesized model outcome, there is no exceptional difference.

The approach taken in this paper towards uncertainty has been to

- Perform a multi-model and multi-observation analysis that summarises what we know at the present moment, using readily available data and methods.

- Apply simple evaluation techniques to readily available data, treating datasets that satisfy evaluation criteria equally and rejecting the others.

- Communicate uncertainties from synthesis. A simple ‘yes’ or ‘no’ is not appropriate in this analysis where there is no clear significant positive or negative trend. Rather, the uncertainties (confidence intervals) and their origin (e.g. natural variability or model spread) are given.

In the long term, a trend in PET only has meaning for crop growth if there is water available for evaporation. Much of eastern Africa is in a water-limited evaporation regime. In the case that irrigation would be locally applied, more water would become available for evaporation, shifting the situation away from a water-limited regime and towards an energy limited regime. A trend in PET seen in our analyses (especially if the analysis using different schemes produces a robust PET trend) could then signify a trend in real evaporation and would therefore be accompanied by an increase in irrigation water demand. Note that irrigation is not accounted for by the models or reanalysis datasets used here.

Previous studies have shown that both the PET scheme and the input data used for calculation of PET can have a large influence on PET values (Trambauer et al., 2014; Wartenburger et al., 2018). We confirm this using the CLM-ERA-PT (Priestley-Taylor), CLM-WFDEI-PT and CLM-ERA-PM (Penman-Monteith) datasets (not shown). In our study regions, PET values are consistently higher when using PM then when using PT. The differences in trends in PET using ERA or WFDEI input or using PT or PM input are sometimes significant. However, comparing study regions, there is no consistency in the difference; in four out of the six regions the PM data shows a higher trend than the PT data and in four out of the six regions WFDEI data shows a higher trend than the ERA data.

There is some evidence that warm spells are increasing in length, particularly in Ethiopia and northern Somalia/Somaliland region (Gebrechorkos et al., 2019), as is the number of consecutive dry days in some parts of eastern Africa, which may have an impact on drought length and increase the rapidity of onset and the intensity of drought (Trenberth et al., 2014). However, the overall impact on crops and food security during long-duration droughts on annual timescales is probably insensitive to this.

It is possible that increasing temperatures have a negative impact on food security during droughts in ways that are beyond the scope of this study, e.g., decreased immunity of livestock, or increased water demand for cooling and water supply (Gebrechorkos et al., 2019, and references therein). In addition, in regions suffering from recent meteorological drought, non-meteorological factors such as increasing population and land-use changes also play a role in worsening the declining vegetation conditions, even after precipitation returns to normal (Pricope et al., 2013).

6 Conclusions

In this first multi-model, multi-method attribution study using several drought estimates in eastern Africa, we address the recurring question on whether increasing global temperatures exacerbate drought. Previous attribution studies for the eastern Africa region have examined drought from a meteorological perspective (precipitation deficit) and have found no clear trends above the noise of natural variability. In this study, we examined trends in eastern African drought from an agricultural perspective (soil moisture) as well as the meteorological perspective (precipitation, temperature and PET) for six regions in eastern Africa. We also investigate whether global-warming driven trends in these meteorological variables can be seen to contribute to trends towards drier soils. In this section, we draw conclusions for each variable in turn and make recommendations.

Out of the four studied variables, soil moisture is most closely related to food security via crop health. In standardized soil moisture data, we found no discernible trends. The uncertainties in trends from model runs were found to be large and there are no long observational runs available. This emphasizes that the use of an ensemble of models is imperative. Due to the large uncertainties in both soil moisture observations and simulations, we conclude that soil moisture cannot be relied upon on its own as a drought indicator and it is therefore important to examine other drought indicators as well. Besides, soil moisture also has a physical lower limit: once the soil is dry it will remain dry. In water limited regions an analysis of precipitation is thus a helpful addition.

Precipitation was found to have a stronger influence than temperature or PET on soil moisture variability, especially in the drier study regions (the significant positive trend in temperature is not reflected by a decrease in soil moisture). However, the confidence intervals on precipitation trend estimations are large and no clear trend is evident.

As expected from the increase in global temperatures, we find significant positive trends in local temperatures in all six regions. The synthesized trend is between 1.0 and 1.3 times the trend in GMST, which corresponds to a local temperature rise of 1.1 to 1.4 degrees from pre-industrial times to 2018. However, the influence of this on annual soil moisture trends appears limited.

PET has a more direct link via evaporation to soil moisture than temperature. The trends in PET are predominantly positive, although in the regions NK and CK the uncertainty in this trend is large. This generally agrees with the positive trends in temperature. Similar to the results for temperature, we do not find strong relations between PET and soil moisture trends. Nevertheless, the results can still be of interest, especially in irrigated regions. Due to large differences in results from different hydrological model runs, we recommend that PET attribution analyses be carried out using an ensemble of hydrological models. These should use various (observational) input datasets and driving GCMs and cover various PET schemes, in order to be representative of the uncertainty surrounding all valid approaches and not bias results towards a particular method.

Whilst it may be preferable to use soil moisture as a drought indicator, observations and simulations of precipitation are more reliable in this region (Coughlan de Perez et al., 2019). Precipitation has a large influence on agricultural droughts and is therefore appropriate to use in attribution studies in eastern Africa, supplementing the analysis of soil moisture. The outcome of previous studies that have focussed on precipitation deficits only (e.g., Philip et al., 2018a; Uhe et al., 2018) are thus still relevant and compare well with our results, that no consistent significant trends on droughts are found.

Finally, communication of the uncertainties in the analyses of soil moisture, precipitation, temperature and PET (and any drought indicators) to policy makers, the media and other stakeholders is crucial. Without insight into the uncertainties in synthesized trends in the different drought indicators, conclusions become meaningless and results can easily be misinterpreted.

Data availability. Almost all time series used in the analysis are available for download under https://climexp.knmi.nl/EastAfrica_timeseries.cgi (last access: 29 April 2019).

Author contributions. Sarah Kew and Sjoukje Philip designed and coordinated the study, analysed all data and led the writing of the manuscript. Mathias Hauser contributed the CLM datasets including PET calculations and substantially contributed to writing. Mike Hobbins produced the RefET dataset and substantially contributed to writing. Niko Wanders and Karin van der Wiel collaborated to create the EC-Earth - PCR-GLOBWB data, including PET calculations and bias correction. Niko Wanders additionally advised on the use and validation of PET and soil moisture data for the analysis of drought. Geert Jan van Oldenborgh contributed analysis tools, monitored progress and contributed to writing. Ted I.E. Veldkamp provided guidance on the use of ISIMIP data and contributed to discussions. Joyce Kimutai and Chris Funk provided local information. Friederike E.L. Otto conceived the idea for the study, monitored development, provided weather@home results and contributed to writing.

Competing interests. We declare that there are no competing interests.

Acknowledgements. We would like to acknowledge funding for this work from the Children's Investment Fund Foundation (CIFF) grant #1805-02753. For their roles in producing, coordinating and making available the ISI-MIP model output, we acknowledge the modelling groups and the ISI-MIP coordination team. We would also like to thank the volunteers running the weather@home models as well as the technical team in OeRC for their support. MERRA-2 data were developed by the Global Modeling and Assimilation Office (GMAO) at NASA Goddard Space Flight Center under funding from the NASA Modeling, Analysis, and Prediction (MAP) program; the data are disseminated through the Goddard Earth Science Data and Information Services Center (GES DISC), preliminary data have been made available thanks to GMAO.

References

Bondeau, A., Smith, P., Zaehle, S., Schaphoff, S., Lucht, W., Cramer, W.and Gerten, D., Lotze-Campen, H., Müller, C., Reichstein, M., and Smith, B.: Modelling the role of agriculture for the 20th century global terrestrial carbon balance, Global Change Biology, 13, 679–706, https://doi.org/10.1111/j.1365-2486.2006.01305.x, 2007.

Collins, W., Bellouin, N., Doutriaux-Boucher, M., Gedney, N., Halloran, P., Hinton, T., Hughes, J., Jones, C., Joshi, M., Liddicoat, S., Martin, G., O'Connor, F., Rae, J., Senior, C., Sitch, S., Totterdell, I., Wiltshire, A., and Woodward, S.: Development and evaluation of an Earth System model, HADGEM2, Geoscientific Model Development, 4, 1051–1075, https://doi.org/10.5194/gmd-4-1051-2011, 2011.

Coughlan de Perez, E., van Aalst, M., Choularton, R., van den Hurk, B., Mason, S., Nissan, H., and Schwager, S.: From rain to famine: assessing the utility of rainfall observations and seasonal forecasts to anticipate food insecurity in East Africa, Food Security, https://doi.org/10.1007/s12571-018-00885-9, 2019.

Dee, D. P., Uppala, S. M., Simmons, A. J., Berrisford, P., Poli, P., Kobayashi, S., Andrae, U., Balmaseda, M. A., Balsamo, G., Bauer, P., Bechtold, P., Beljaars, A. C. M., van de Berg, L., Bidlot, J., Bormann, N., Delsol, C., Dragani, R., Fuentes, M., Geer, A. J., Haimberger, L., Healy, S. B., Hersbach, H., Hólm, E. V., Isaksen, L., Kållberg, P., Köhler, M., Matricardi, M., McNally, A. P., Monge-Sanz, B. M., Morcrette, J.-J., Park, B.-K., Peubey, C., de Rosnay, P., Tavolato, C., Thépaut, J.-N., and Vitart, F.: The ERA-Interim reanalysis: Configuration and performance of the data assimilation system, Quart. J. Roy. Meteor. Soc., 137, 553–597, https://doi.org/10.1002/qj.828, 2011.

Dufresne, J.-L., Foujols, M.-A., Denvil, S., Caubel, A., Marti, O., Aumont, O., Balkanski, Y., Bekki, S., Bellenger, H., Benshila, R., Bony, S., Bopp, L., Braconnot, P., Brockmann, P., Cadule, P., Cheruy, F., Codron, F., Cozic, A., Cugnet, D., de Noblet, N., Duvel, J.-P., Ethé, C., Fairhead, L., Fichefet, T., Flavoni, S., Friedlingstein, P., Grandpeix, J.-Y., Guez, L., Guilyardi, E., Hauglustaine, D., Hourdin, F., Idelkadi, A., Ghattas, J., Joussaume, S., Kageyama, M., Krinner, G., Labetoulle, S., Lahellec, A., Lefebvre, M.-P., Lefevre, F., Levy, C., Li, Z. X., Lloyd, J., Lott, F., Madec, G., Mancip, M., Marchand, M., Masson, S., Meurdesoif, Y., Mignot, J., Musat, I., Parouty, S., Polcher, J., Rio, C., Schulz, M., Swingedouw, D., Szopa, S., Talandier, C., Terray, P., Viovy, N., and Vuichard, N.: Climate change projections using the IPSL-CM5 Earth System Model: from CMIP3 to CMIP5, Climate Dynamics, 40, 2123–2165, https://doi.org/10.1007/s00382-012-1636-1, 2013.

Dunne, J. P., John, J. G., Adcroft, A. J., Griffies, S. M., Hallberg, R. W., Shevliakova, E., Stouffer, R. J., Cooke, W., Dunne, K. A., Harrison, M. J., Krasting, J. P., Malyshev, S. L., Milly, P. C. D., Phillipps, P. J., Sentman, L. T., Samuels, B. L., Spelman, M. J., Winton, M., Wittenberg, A. T., and Zadeh, N.: GFDL's ESM2 Global Coupled Climate—Carbon Earth System Models. Part I: Physical Formulation and Baseline Simulation Characteristics, Journal of Climate, 25, 6646–6665, https://doi.org/10.1175/JCLI-D-11-00560.1, 2012.

Dunne, J. P., John, J. G., Shevliakova, E., Stouffer, R. J., Krasting, J. P., Malyshev, S. L., Milly, P. C. D., Sentman, L. T., Adcroft, A. J., Cooke, W., Dunne, K. A., Griffies, S. M., Hallberg, R. W., Harrison, M. J., Levy, H., Wittenberg, A. T., Phillips, P. J., and Zadeh, N.: GFDL's ESM2 Global Coupled Climate—Carbon Earth System Models. Part II: Carbon System Formulation and Baseline Simulation Characteristics, Journal of Climate, 26, 2247–2267, https://doi.org/10.1175/JCLI-D-12-00150.1, 2013.

Fan, Z.-X. and Thomas, A.: Decadal changes of reference crop evapotranspiration attribution: Spatial and temporal variability over China 1960–2011, Journal of Hydrology, 560, 461 – 470, https://doi.org/https://doi.org/10.1016/j.jhydrol.2018.02.080, 2018.

Funk, C., Nicholson, S. E., Landsfeld, M., Klotter, D., Peterson, P., and Harrison, L.: The centennial trends greater horn of Africa precipitation dataset, Scientific data, 2, 150 050, https://doi.org/10.1038/sdata.2015.50, 2015.

Gebrechorkos, S. H., Hülsmann, S., and Bernhofer, C.: Changes in temperature and precipitation extremes in Ethiopia, Kenya, and Tanzania, International Journal of Climatology, 39, 18–30, https://doi.org/10.1002/joc.5777, 2019.

Guillod, B. P., Jones, R. G., Bowery, A., Haustein, K., Massey, N. R., Mitchell, D. M., Otto, F. E. L., Sparrow, S. N., Uhe, P., Wallom, D. C. H., Wilson, S., and Allen, M. R.: weather@home 2: validation of an improved global–regional climate modelling system, Geoscientific Model Development, 10, 1849–1872, https://doi.org/10.5194/gmd-10-1849-2017, 2017.

Hanasaki, N., Kanae, S., Oki, T., Masuda, K., Motoya, K., Shirakawa, N., Shen, Y., and Tanaka, K.: An integrated model for the assessment of global water resources – Part 1: Model description and input meteorological forcing, Hydrology and Earth System Sciences, 12, 1007–1025, https://doi.org/10.5194/hess-12-1007-2008, 2008a.

Hanasaki, N., Kanae, S., Oki, T., Masuda, K., Motoya, K., Shirakawa, N., Shen, Y., and Tanaka, K.: An integrated model for the assessment of global water resources – Part 2: Applications and assessments, Hydrology and Earth System Sciences, 12, 1027–1037, https://doi.org/10.5194/hess-12-1027-2008, 2008b.

Hansen, J., Ruedy, R., Sato, M., and Lo, K.: Global Surface Temperature Change, Rev. Geophys., 48, RG4004, https://doi.org/DOI 10.1029/2010RG000345, 2010.

Harris, I., Jones, P., Osborn, T., and Lister, D.: Updated high-resolution grids of monthly climatic observations – the CRU TS3.10 Dataset, International Journal of Climatology, 34, 623–642, https://doi.org/10.1002/joc.3711, 2014.

Hazeleger, W., Wang, X., Severijns, C., Ştefănescu, S., Bintanja, R., Sterl, A., Wyser, K., Semmler, T., Yang, S., Van den Hurk, B., et al.: EC-Earth V2. 2: description and validation of a new seamless earth system prediction model, Climate dynamics, 39, 2611–2629, 2012.

Hempel, S., Frieler, K., Warszawski, L., Schewe, J., and Piontek, F.: A trend-preserving bias correction — the ISI-MIP approach, Earth System Dynamics, 4, 219–236, https://doi.org/10.5194/esd-4-219-2013, 2013.

Hobbins, M. T., Shukla, S., McNally, A. L., McEvoy, D. J., Huntington, J. L., Husak, G. J., Funk, C. C., Senay, G. B., Verdin, J. P., Jansma, T., and Dewes, C. F.: What role does evaporative demand play in driving drought in Africa?, AGU Fall Meeting Abstracts, San Francisco, CA, abstract GC43F-02, 2016.

Hobbins, M. T., Dewes, C. F., McEvoy, D. J., Shukla, S., Harrison, L. S., Blakeley, S. L., McNally, A. L., and Verdin, J. P.: A new global reference evapotranspiration reanalysis forced by MERRA2: Opportunities for famine early warning, drought attribution, and improving drought monitoring, in: proceedings of the 98th annual meeting, American Meteorological Society Annual Meeting, Austin, TX, 2018.

James, R., Washington, R., Abiodun, B., Kay, G., Mutemi, J., Pokam, W., Hart, N., Artan, G., and Senior, C.: Evaluating Climate Models with an African Lens, Bulletin of the American Meteorological Society, 99, 313–336, https://doi.org/10.1175/BAMS-D-16-0090.1, 2018.

Jones, C. D., Hughes, J., Bellouin, N., Hardimann, S., Jones, G., Knight, J., Liddicoat, S., O'Connor, F., Andres, R. J., Bell, C., Boo, K.-O., Bozzo, A., Butchart, N., Cadule, P., Corbin, K., Doutriaux-Boucher, M., Friedlingstein, P., Gornall, J., Gray, L., Halloran, P., Hurtt, G., Ingram, W., Lamarque, J.-F., Law, R., Meinshausen, M., Osprey, S., Palin, E. J., Parsons Chini, L., Raddatz, T., Sanderson, M. G., Sellar, A. A., Schurer, A., Valdes, P., Wood, N., Woodward, S., Yoshioka, M., and Zerroukat, M.: The HadGEM2-ES implementation of CMIP5 centennial simulations, Geosci. Model Dev., 4, 543–570, https://doi.org/10.5194/gmd-4-543-2011, 2011.

Kew, S. F., Philip, S. Y., van Oldenborgh, G. J., van der Schrier, G., Otto, F. E., and Vautard, R.: The Exceptional Summer Heat Wave in Southern Europe 2017, Bulletin of the American Meteorological Society, 100, S49–S53, https://doi.org/10.1175/BAMS-D-18-0109.1, 2019.

Lawrence, D. M., Oleson, K. W., Flanner, M. G., Thornton, P. E., Swenson, S. C., Lawrence, P. J., Zeng, X., Yang, Z.-L., Levis, S., Sakaguchi, K., Bonan, G. B., and Slater, A. G.: Parameterization improvements and functional and structural advances in Version 4 of the Community Land Model, Journal of Advances in Modeling Earth Systems, 3, https://doi.org/10.1029/2011MS00045, 2011.

Li, Z., Chen, Y., Yang, J., and Wang, Y.: Potential evapotranspiration and its attribution over the past 50 years in the arid region of Northwest China, Hydrological Processes, 28, 1025–1031, https://doi.org/10.1002/hyp.9643, 2014.

Liu, D. and Mishra, A. K.: Performance of AMSR_E soil moisture data assimilation in CLM4.5 model for monitoring hydrologic fluxes at global scale, Journal of Hydrology, 547, 67 – 79, https://doi.org/10.1016/j.jhydrol.2017.01.036, 2017.

Manning, C., Widmann, M., Bevacqua, E., van Loon, A. F., Maraun, D., and Vrac, M.: Soil Moisture Drought in Europe: A Compound Event of Precipitation and Potential Evapotranspiration on Multiple Time Scales, Journal of Hydrometeorology, 19, 1255–1271, https://doi.org/10.1175/JHM-D-18-0017.1, 2018.

Massey, N., Jones, R., Otto, F. E. L., Aina, T., Wilson, S., Murphy, J. M., Hassell, D., Yamazaki, Y. H., and Allen, M. R.: weather@home—development and validation of a very large ensemble modelling system for probabilistic event attribution, Quarterly Journal of the Royal Meteorological Society, 141, 1528–1545, https://doi.org/10.1002/qj.2455, 2015.

McNally, A., Shukla, S., Arsenault, K. R., Wang, S., Peters-Lidard, C. D., and Verdin, J. P.: Evaluating ESA CCI soil moisture in East Africa, International Journal of Applied Earth Observation and Geoinformation, 48, 96–109, https://doi.org/https://doi.org/10.1016/j.jag.2016.01.001, 2016.

McNally, A., Arsenault, K., Kumar, S., Shukla, S., Peterson, P., Wang, S., Funk, C., Peters-Lidard, C. D., and Verdin, J. P.: A land data assimilation system for sub-Saharan Africa food and water security applications, Scientific Data, 4, 170 012, https://doi.org/10.1038/sdata.2017.12, 2017.

Müller Schmied, H., Adam, L., Eisner, S., Fink, G., Flörke, M., Kim, H., Oki, T., Portmann, F. T., Reinecke, R., Riedel, C., Song, Q., Zhang, J., and Döll, P.: Variations of global and continental water balance components as impacted by climate forcing uncertainty and human water use, Hydrology and Earth System Sciences, 20, 2877–2898, https://doi.org/10.5194/hess-20-2877-2016, 2016.

Obada, E., Alamou, E. A., Chabi, A., Zandagba, J., and Afouda, A.: Trends and Changes in Recent and Future Penman-Monteith Potential Evapotranspiration in Benin (West Africa), Hydrology, 4, https://doi.org/10.3390/hydrology4030038, 2017.

Oleson, K. W., Lawrence, D. M., Bonan, G. B., Flanner, M. G., Kluzek, E., Lawrence, P. J., Levis, S., Swenson, S. C., Thornton, P. E., Dai, A., Decker, M., DIckinson, R., Feddema, J., Heald, C. L., Hoffman, F., Lamarque, J. F., Mahowald, N., Niu, G., Qian, T., Randerson, J., Running, S., Sakaguchi, K., Slater, A., Stockli, R., Wang, A., Yang, Z., Zeng, X., and Zeng, X.: Technical description of version 4.0 of the Community Land Model, NCAR Technical Note 257, NCAR, https://doi.org/doi:10.5065/D6FB50WZ, 2010.

Philip, S., Kew, S. F., van Oldenborgh, G. J., Otto, F., O'Keefe, S., Haustein, K., King, A., Zegeye, A., Eshetu, Z., Hailemariam, K., Singh, R., Jjemba, E., Funk, C., and Cullen, H.: Attribution Analysis of the Ethiopian Drought of 2015, Journal of Climate, 31, 2465–2486, https://doi.org/10.1175/JCLI-D-17-0274.1, 2018a.

Philip, S. Y., Kew, S. F., Hauser, M., Guillod, B. P., Teuling, A. J., Whan, K., Uhe, P., and van Oldenborgh, G. J.: Western US high June 2015 temperatures and their relation to global warming and soil moisture, Clim. Dyn., 50, 2587–2601, https://doi.org/10.1007/s00382-017-3759-x, 2018b.

Philip, S. Y., Kew, S. F., van Oldenborgh, G. J., Otto, F. E. L., Vautard, R., van der Wiel, K., King, A., L., F., Arrighi, J., Singh, R., and van Aalst, M.: A protocol for probabilistic extreme event attribution analyses, in prep., 2019.

Pricope, N. G., Husak, G., Lopez-Carr, D., Funk, C., and Michaelsen, J.: The climate-population nexus in the East African Horn: Emerging degradation trends in rangeland and pastoral livelihood zones, Global Environmental Change, 23, 1525 – 1541, https://doi.org/https://doi.org/10.1016/j.gloenvcha.2013.10.002, 2013.

Prudhomme, C., Giuntoli, I., Robinson, E. L., Clark, D. B., Arnell, N. W., Dankers, R., Fekete, B. M., Franssen, W., Gerten, D., Gosling, S. N., Hagemann, S., Hannah, D. M., Kim, H., Masaki, Y., Satoh, Y., Stacke, T., Wada, Y., and Wisser, D.: Hydrological droughts in the 21st century, hotspots and uncertainties from a global multimodel ensemble experiment, Proceedings of the National Academy of Sciences, 111, 3262–3267, https://doi.org/10.1073/pnas.1222473110, 2014.

Rohde, R., Curry, J., Groom, D., Jacobsen, R., Muller, R. A., Perlmutter, S., Wickham, A. R. C., and Mosher, S.: Berkeley Earth Temperature Averaging Process, Geoinfor Geostat An Overview, 1:2, https://doi.org/10.4172/2327-4581.1000103, 2013a.

Rohde, R., Muller, R., Jacobsen, R., Muller, E., and Perlmutter, S.: A New Estimate of the Average Earth Surface Land Temperature Spanning 1753 to 2011, Geoinfor Geostat An Overview, 1:1, https://doi.org/10.4172/2327-4581.1000101, 2013b.

Rost, S., Gerten, D., Bondeau, A., Lucht, W., Rohwer, J., and Schaphoff, S.: Agricultural green and blue water consumption and its influence on the global water system, Water Resources Research, 44, https://doi.org/10.1029/2007WR006331, 2008.

Rowell, D. P., Booth, B. B. B., Nicholson, S. E., and Good, P.: Reconciling Past and Future Rainfall Trends over East Africa, Journal of Climate, 28, 9768–9788, https://doi.org/10.1175/JCLI-D-15-0140.1, 2015.

Schaphoff, S., Heyder, U., Ostberg, S., Gerten, D., Heinke, J., and Lucht, W.: Contribution of permafrost soils to the global carbon budget, Environmental Research Letters, 8, 014 026, https://doi.org/10.1088/1748-9326/8/1/014026, 2013.

Shongwe, M. E., van Oldenborgh, G. J., van den Hurk, B. J. J. M., and van Aalst, M. K.: Projected Changes in Mean and Extreme Precipitation in Africa under Global Warming. Part II: East Africa, J. Climate, 24, 3718–3733, https://doi.org/10.1175/2010JCLI2883.1, 2011.

Sippel, S., Otto, F. E. L., Flach, M., and van Oldenborgh, G. J.: The Role of Anthropogenic Warming in 2015 Central European Heat Waves, Bull. Amer. Met. Soc., 97, S51–S56, https://doi.org/10.1175/BAMS-D-16-0150.1, 2016.

Sutanudjaja, E. H., van Beek, R., Wanders, N., Wada, Y., Bosmans, J. H. C., Drost, N., van der Ent, R. J., de Graaf, I. E. M., Hoch, J. M., de Jong, K., Karssenberg, D., López López, P., Peßenteiner, S., Schmitz, O., Straatsma, M. W., Vannametee, E., Wisser, D., and Bierkens, M. F. P.: PCR-GLOBWB 2: a 5 arcmin global hydrological and water resources model, Geoscientific Model Development, 11, 2429–2453, https://doi.org/10.5194/gmd-11-2429-2018, 2018.

Trambauer, P., Dutra, E., Maskey, S., Werner, M., Pappenberger, F., van Beek, L. P. H., and Uhlenbrook, S.: Comparison of different evaporation estimates over the African continent, Hydrology and Earth System Sciences, 18, 193–212, https://doi.org/10.5194/hess-18-193-2014, 2014.

Trenberth, K. E., Dai, A., Van Der Schrier, G., Jones, P. D., Barichivich, J., Briffa, K. R., and Sheffield, J.: Global warming and changes in drought, Nature Climate Change, 4, 17, 2014.

Uhe, P., Philip, S., Kew, S., Shah, K., Kimutai, J., Mwangi, E., van Oldenborgh, G. J., Singh, R., Arrighi, J., Jjemba, E., Cullen, H., and Otto, F.: Attributing drivers of the 2016 Kenyan drought, International Journal of Climatology, 38, e554–e568, https://doi.org/10.1002/joc.5389, 2018.

van der Wiel, K., Kapnick, S. B., van Oldenborgh, G. J., Whan, K., Philip, S. Y., Vecchi, G. A., Singh, R. K., Arrighi, J., and Cullen, H.: Rapid attribution of the August 2016 flood-inducing extreme precipitation in south Louisiana to climate change, Hydrol. Earth Syst. Sci., 21, 897–921, https://doi.org/10.5194/hess-21-897-2017, 2017.

van Loon, A., Gleeson, T., Clark, J., Van Dijk, A., Stahl, K., Hannaford, J., Di Baldassarre, G., Teuling, A., Tallaksen, L., Uijlenhoet, R., Hannah, D., Sheffield, J., Svoboda, M., Verbeiren, B., Wagener, T., Rangecroft, S., Wanders, N., and Van Lanen, H.: Drought in the Anthropocene, Nature Geoscience, 9, 89–91, https://doi.org/10.1038/ngeo2646, 2016.

van Oldenborgh, G. J., Philip, S. Y., Kew, S. F., van Weele, M., Uhe, P., Otto, F. E. L., Singh, R., Pai, I., Cullen, H., and AchutaRao, K.: Extreme heat in India and anthropogenic climate change, Natural Hazards and Earth System Sciences, 18, 365–381, https://doi.org/10.5194/nhess-18-365-2018, 2018.

van Oldenborgh, G. J., Otto, F. E. L., Vautard, R., van der Wiel, K., Kew, S., Philip, S., King, A., L., F., Arrighi, J., Singh, R., and van Aalst, M.: Pathways and pitfalls in extreme event attribution, in review for Bulletin of the American Meteorological Society, 2019.

Wada, Y., Wisser, D., Eisner, S., Flörke, M., Gerten, D., Haddeland, I., Hanasaki, N., Masaki, Y., Portmann, F. T., Stacke, T., et al.: Multimodel projections and uncertainties of irrigation water demand under climate change, Geophysical Research Letters, 40, 4626–4632, 2013.

Wartenburger, R., Seneviratne, S. I., Hirschi, M., Chang, J., Ciais, P., Deryng, D., Elliott, J., Folberth, C., Gosling, S. N., Gudmundsson, L., Henrot, A.-J., Hickler, T., Ito, A., Khabarov, N., Kim, H., Leng, G., Liu, J., Liu, X., Masaki, Y., Morfopoulos, C., Müller, C., Schmied, H. M., Nishina, K., Orth, R., Pokhrel, Y., Pugh, T. A. M., Satoh, Y., Schaphoff, S., Schmid, E., Sheffield, J., Stacke, T., Steinkamp, J., Tang, Q., Thiery, W., Wada, Y., Wang, X., Weedon, G. P., Yang, H., and Zhou, T.: Evapotranspiration simulations in ISIMIP2a—Evaluation of spatio-temporal characteristics with a comprehensive ensemble of independent datasets, Environmental Research Letters, 13, 075 001, https://doi.org/10.1088/1748-9326/aac4bb, 2018.

Watanabe, M., Suzuki, T., O'ishi, R., Komuro, Y., Watanabe, S., Emori, S., Takemura, T., Chikira, M., Ogura, T., Sekiguchi, M., Takata, K., Yamazaki, D., Yokohata, T., Nozawa, T., Hasumi, H., Tatebe, H., and Kimoto, M.: Improved Climate Simulation by MIROC5: Mean States, Variability, and Climate Sensitivity, Journal of Climate, 23, 6312–6335, https://doi.org/10.1175/2010JCLI3679.1, 2010.

Weedon, G. P., Balsamo, G., Bellouin, N., Gomes, S., Best, M. J., and Viterbo, P.: The WFDEI meteorological forcing data set: WATCH Forcing Data methodology applied to ERA-Interim reanalysis data, Water Resources Research, 50, 7505–7514, https://doi.org/10.1002/2014WR015638, 2014.

Wilhite, D. and Glantz, M.: Understanding the Drought Phenomenon: The Role of Definitions, Water International, 10, 111–120, 1985.

Yin, Y., Wu, S., Chen, G., and Dai, E.: Attribution analyses of potential evapotranspiration changes in China since the 1960s, Theoretical and Applied Climatology, 101, 19–28, https://doi.org/10.1007/s00704-009-0197-7, 2010.